Darcy–Brinkman–Forchheimer flow over irregular domain using finite elements method

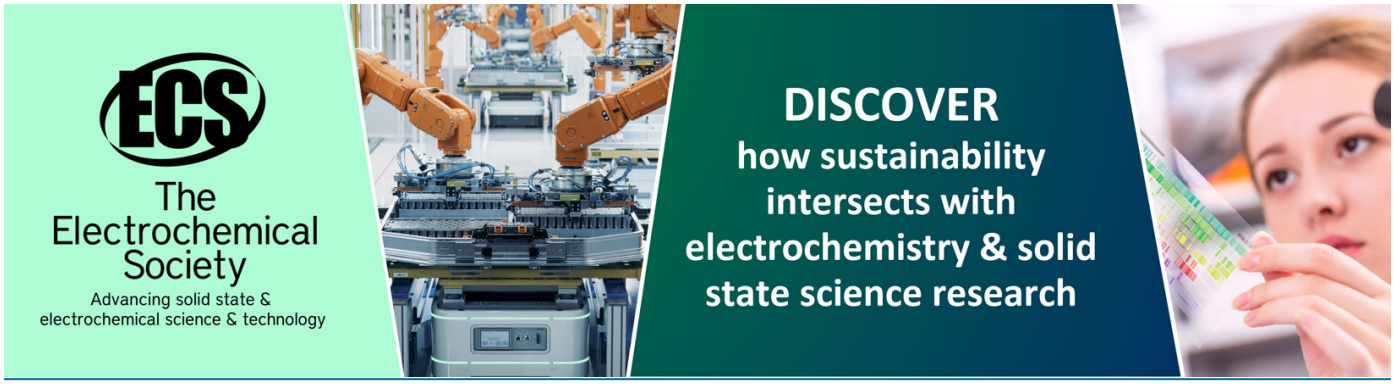

IOP Conf. Series: Materials Science and Engineering **577** (2019) 012158 doi:10.1088/1757-899X/577/1/012158

Darcy–Brinkman–Forchheimer flow over irregular domain using finite elements method

K. Murali, V. Kesavulu Naidu and B. Venkatesh
Department of Mathematics, Amrita School of Engineering, Bengaluru, Amrita Vishwa Vidyapeetham, India

E-mail: k_murali@blr.amrita.edu

Abstract. The finite element method of solution with curved triangles to solve the three-dimensional, fully-developed Darcy–Brinkman–Forchheimer flow equation in channel with curved side is solved using quasi-linearization and Gauss-Seidel iteration method. Exhaustive numerical computation and numerical experimentation reveals the parameters' influence on the velocity distributions.. A salient feature of the method adopted in the present paper is that it ensures that the errors are almost equally distributed among all the nodes. It is found that the irregular cross-section channel with upward concave boundary decelerates the flow. Numerical experimentation involved different order curved triangular elements and extensive computation revealed that the quintic order curved triangular element yields the desired solution to an accuracy of 10^{-5}. The finite element method is found to be very effective in capturing boundary and inertia effects in the three-dimensional, fully-developed flow through porous media. Further, it succeeds in giving the required solution for large values of Forchheimer number when shooting method fails to do so. The method can be easily employed in any other irregular cross-section channel.

1. Introduction

The importance of porous media in practical applications is well known in the literature (see Nield and Bejan [1], Vafai [2], Rudraiah et al. [3]). Many eminent researchers advocated to have boundary and inertia effects in flow equations of porous media. The recent work of Skjetne and Auriault [4] provides new insights on steady, non-linear flow in porous media. Also the authors Calmidi and Mahajan [5] presented the non-linear, non-Darcy equation as an excellent candidate for description of flow in metal foam porous media. The work of Khaled and Vafai [6] take us from extra-corporeal application situations into corporeal flows. Their [6] work presents a non-linear flow model for high perfused skeletal tissues. In all these works, and many more, high flow rate and /or high permeability in porous media warrants the quantification of the departure from Darcy's law in terms of Brinkman friction and super-linear drag, the former arising due to solid boundaries and the latter caused by form drag due to the solid matrix. The analytical solution of upstream velocity profile for nonlinear flow model in porous channel is determined in Ramos [7]. Restricting our attention to uni-directional flows, here we may recall two extremely important works of Vafai and Kim [8], and Nield et al. [9] that deal with forced convection in a channel filled with a porous medium. A steady, uni-directional, non-linear, non-Darcy flow was assumed in these works. The above two works concern exact solutions of the non-linear two-point boundary-value problem arising in the study. The non-linearity in the governing quasi-linear differential equation is a quadratic function of velocity. In literature, the nomenclature attached with this friction is either after the name of Forchheimer [10] or Ergun [11]. In

so far as the Darcy friction and viscous shear is concerned, there is a need to have two viscosities (actual fluid viscosity and effective viscosity) in the equation (Lauriat and Prasad [12] and Givler and Altobelli [13]). In the present problem we consider the non-Darcy effects due to both boundary and inertia. Poulikakos and Renken [14] performed a numerical study of boundary and inertial effects on porous medium flow and heat transfer. Parang and Keyhani [15] studied the effect of boundary and inertia effects on mixed convection in an annular region. Hooman [16], Hooman and Gurgenci [17], Sharma et al. [18] and Allan and Hamdan [19] have recent numerical works on non-linear flow model in porous media. In the most recent works, natural convective flow and heat transfer of nanofluids in different channels with porous matrix is investigated with the help of Darcy-Forchheimer-Brinkman model[32,33].

In spite of there being works reporting solution of the Darcy–Brinkman–Forchheimer equation for fully developed two-dimensional rectangular channel, the need to consider irregular cross-section porous channels in many applications necessitates to revisit the problem[30]. In article curved elements are employed with the basis functions chosen to fit the curved boundary of the irregular cross-section. Practical problems involving complex curved boundary domains pose so much computational hardship for finite difference and classical finite element computations. Curved triangular elements with one curved side and two straight sides can map the curved domains better than using the three straight sided triangular elements. Ergatoudis et al. [20] has discussed about the use of curved triangular elements in structural mechanics. The use of parabolic arcs, the derivation of the iso-parametric transformation involving the one curved side and two straight sides are given in the works of Zienkiewicz [21], Macleod and Mitchell [22], Rathod and Karim [23, 24], and Rathod et al. [25].

2. Mathematical formulation

In the case of steady state fully developed flow, we have unidirectional flow in the z -direction inside the tubes in porous channels involving both regular and irregular boundary(see Figs.1a), the Darcy–Brinkman–Forchheimer momentum equation with velocity $u(x, y)$ is

$$\mu'\left(\frac{\partial^2 u}{\partial x^2}+\frac{\partial^2 u}{\partial y^2}\right)-\frac{\mu}{\mathrm{K}}u-\frac{\rho C_b}{\sqrt{K}}u^2=\frac{dp}{dz}. \tag{1}$$

Non-dimensionalise Eq. (1) using the following definitions:

$$X=\frac{x}{h},\ Y=\frac{y}{h},\ Z=\frac{z}{h},\ U=\frac{u}{u_R\left(-\frac{dP}{dZ}\right)},\ P=\frac{p\,h}{\mu u_R\left(-\frac{dP}{dZ}\right)}. \tag{2}$$

Substituting Eq. (2) in the Eq. (1), we get

$$\left(\frac{\partial^2 U}{\partial X^2}+\frac{\partial^2 U}{\partial Y^2}\right)-\Lambda\sigma^2 U-F\,U^2=-\Lambda, \tag{3}$$

where, $\Lambda=\dfrac{\mu}{\mu'}$ viscosity ratio (Brinkman number), $\sigma^2=\dfrac{h^2}{\mathrm{K}}$ (porous parameter), $\mathrm{Re}=-\dfrac{u_R h}{\nu}\dfrac{dP}{dZ}$ (Reynolds number) and $F=\Lambda C_b\,\mathrm{Re}\,\sigma$ (Forchheimer number).

At this juncture we note that the Brinkman and Darcy numbers used here are actually the inverse of the classical definitions. The definition of the Brinkman, Darcy and Forchheimer numbers in Eq. (3) is the same as that used in Nield et al. [9]. Equation (1)'s non-dimensional form is Eq. (3). We solve Eq. (3) subject to the following boundary condition:

$$U = 0 \text{ on } \partial\Omega, \tag{4}$$

where $\partial\Omega$ is the boundary of the cross-section Ω (see Figs. 1b).

The field problem governed by Eqs. (3) and (4) is solved by using the Galerkin weighted residual method (see Bathe [26], Zienkiewicz et al. [27] and Bhatti [28]. The boundary Ω in Figs. 1b is partitioned into many triangular elements Ω_e as shown in Fig. 6 so the boundary $\partial\Omega$ is also divided accordingly. Quadratic, cubic, quartic and quintic order curved triangular elements with one curved side and two straight sides are used in the present paper (see Figs 2-7). The function U within the curved triangular element is given as

$$U = \sum_{i=1}^{NP} N_i(\xi,\eta) U_i, \tag{5}$$

where U_i's are unknown values of U and N_i's are Lagrange interpolants or shape functions for the standard triangular element and

$$NP = \begin{cases} 6 & \text{for } 6-\text{node quadratic triangular element,} \\ 10 & \text{for } 10-\text{node cubic triangular element,} \\ 15 & \text{for } 15-\text{node quartic triangular element,} \\ 21 & \text{for } 21-\text{node quintic triangular element.} \end{cases}$$

The point transformation for the curved triangular elements with one curved side and two straight sides can be expressed in terms of the four points $t_i\,(i=1,2,3,4)$ is given by

$$t(\xi,\eta) = t_3 + (t_1 - t_3)\xi + (t_2 - t_3)\eta + \frac{n}{(n-1)}[nt_4 - ((n-1)t_2 + t_1)]\xi\eta, \quad (t = X, Y), \tag{6}$$

where $n = 2,3,4,5$ for the quadratic, cubic, quartic and quintic curved triangular elements respectively for Figs. 2–5. The detailed derivations are shown in the works of Rathod et al. [25].
By using the transformation in Eq. (6), the Jacobian $J(\xi,\eta)$ can be expressed as:

$$J(\xi,\eta) = \frac{\partial(X,Y)}{\partial(\xi,\eta)} = \frac{\partial X}{\partial\xi}\frac{\partial Y}{\partial\eta} - \frac{\partial X}{\partial\eta}\frac{\partial Y}{\partial\xi}. \tag{7}$$

Finite element equations for each of the triangular elements for Eq. (3) is obtain by using the Galerkin method of weighted residuals, we get following finite element equation for each element as

$$[D^e + G^e]_{NP\times NP}.\{U^e\}_{NP\times 1} = \{B^e\}_{NP\times 1} - \{E^e\}_{NP} \quad \text{or} \quad D^e_{i,j}\,U^e_{i,j} + G^e_{i,j}\,U^e_{i,j} = B^e_i - E^e_i, \tag{8a}$$

where

$$D^e_{i,j} = \iint_{\Omega_e}\left(\frac{\partial N_i}{\partial X}\frac{\partial N_j}{\partial X} + \frac{\partial N_i}{\partial Y}\frac{\partial N_j}{\partial Y}\right)dXdY = D^{i,j}_{X,X} + D^{i,j}_{Y,Y}, \tag{8b}$$

$$D^{i,j}_{X,X} = \int_{\xi=0}^{1}\int_{\eta=0}^{1-\xi}\frac{1}{J^e}\left(\frac{\partial N_i}{\partial\xi}\frac{\partial Y}{\partial\eta} - \frac{\partial N_i}{\partial\eta}\frac{\partial Y}{\partial\xi}\right)\left(\frac{\partial N_j}{\partial\xi}\frac{\partial Y}{\partial\eta} - \frac{\partial N_j}{\partial\eta}\frac{\partial Y}{\partial\xi}\right)d\eta\,d\xi,$$

$$D_{Y,Y}^{i,j} = \int_{\xi=0}^{1}\int_{\eta=0}^{1-\xi} \frac{1}{J^e}\left(-\frac{\partial N_i}{\partial \xi}\frac{\partial X}{\partial \eta}+\frac{\partial N_i}{\partial \eta}\frac{\partial X}{\partial \xi}\right)\left(-\frac{\partial N_j}{\partial \xi}\frac{\partial X}{\partial \eta}+\frac{\partial N_j}{\partial \eta}\frac{\partial X}{\partial \xi}\right)d\eta d\xi ,$$

$$G_{i,j}^{e} = \iint_{\Omega_e} \Lambda\sigma^2 N_i\, N_j\, dXdY = \int_{\xi=0}^{1}\int_{\eta=0}^{1-\xi} \Lambda\sigma^2 N_i\, N_j\, J^e d\eta d\xi , \tag{8c}$$

$$B_i^e = \iint_{\Omega_e} \Lambda N_i\, dXdY = \int_{\xi=0}^{1}\int_{\eta=0}^{1-\xi} \Lambda N_i\, J^e d\eta d\xi , \tag{8d}$$

$$E_i^e = \iint_{\Omega_e}\left(F\ N_i\left(\sum_{j=1}^{NP} N_j U_j\right)^2\right)dXdY = \int_{\xi=0}^{1}\int_{\eta=0}^{1-\xi}\left(F\ N_i\left(\sum_{j=1}^{NP} N_j U_j\right)^2\right)\left|J^e\right| d\eta d\xi . \tag{8e}$$

i and j takes the values from 1 to NP in the Eq. (8). Using Gauss quadrature rules over standard given in Rathod et al. [30,31], the Eq. (8) integrals can be numerically evaluated.

Assembling is done after matrices D^e, G^e, B^e and E^e related to each element are calculated to get the global matrices D, G, B and E related to the whole physical domain. On imposing the boundary conditions , we get

$$[D+G]_{m\times m}.\{U\}_{m\times 1} = \{B\}_{m\times 1} - \{E\}_{m\times 1} \text{ or } \qquad [H]_{m\times m}.\{U\}_{m\times 1} = \{B\}_{m\times 1} - \{E\}_{m\times 1}, \tag{10}$$

where

$$H_{i,j} = D_{i,j} + G_{i,j} .$$

We get a system of *m* nonlinear algebraic equations in *m* unknown interior velocities U_i in Eq. (10). We solve the Eq. (10) by first converting it to quasi-linearized system. Eq. (10) and then applying Gauss-Seidel iterative formula. Eq. (10) in the quasi-linearized form for $m = 3$ can be written as:

$$\begin{aligned}
&\left(H_{1,1} + E_1 U_1\right)U_1 + H_{1,2}U_2 + H_{1,3}U_3 = B_1,\\
&H_{2,1}U_1 + \left(H_{2,2} + E_2 U_2\right)U_2 + H_{2,3}U_3 = B_2,\\
&H_{3,1}U_1 + H_{3,2}U_2 + \left(H_{3,3} + E_3 U_3\right)U_3 = B_3 .
\end{aligned} \tag{11}$$

Gauss-Seidel iterative formula for solving Eq. (11) can be rewritten as:

$$\begin{aligned}
U_1^{(k)} &= \frac{1}{\left(H_{1,1} + E_1 U_1^{(k-1)}\right)}\left(B_1 - H_{1,2}U_2^{(k-1)} - H_{1,3}U_3^{(k-1)}\right),\\
U_2^{(k)} &= \frac{1}{\left(H_{2,2} + E_2 U_2^{(k-1)}\right)}\left(B_2 - H_{2,1}U_1^{(k)} - H_{2,3}U_3^{(k-1)}\right),\\
U_3^{(k)} &= \frac{1}{\left(H_{3,3} + E_3 U_3^{(k-1)}\right)}\left(B_3 - H_{3,1}U_1^{(k)} - H_{3,2}U_2^{(k)}\right).
\end{aligned} \tag{12}$$

The convergence criteria can be set as:

$$U_i^k - U_i^{k-1} \le \text{Tol} , \tag{13}$$

where k is the iterative number and Tol is an acceptable tolerance.

3. Results and discussion

The present work intends to propose the finite element method for solving a non-linear, non-Darcy equation with quadratic drag. Before we embark on a discussion of the solution we note here that the definition of Brinkman and Darcy numbers as used in the paper is the inverse of the classical

definitions. High-porosity channels of regular or irregular cross-sections are considered for investigating Newtonian fluid flow through it. The boundary effects of the physical problems involving the curved domains are not easily captured by the finite difference and classical finite element method with straight sided triangular elements. Hence, the curved triangular elements with one curved side and two straight sides are used in solving the field problems involving curved boundaries. In solving the present partial differential equation, we get the product of the global derivatives as in Eqs. (8b)&(8c). The higher order bivariate Jacobians in the denominators of the integrand in Eq. (8c) imposes the more numerical integration cost in getting the accurate numerical values. The prime reason for the huge computational cost escalation in evaluating Eq. (8c) is contributed by higher order bivariate Jacobians of the iso-parametric point transformations for cubic, quartic and quintic order triangular elements, since three, four and five are the orders of the iso-parametric point transformations for the cubic, quartic and quintic order curved triangular elements. So, the huge computational burden can be reduced by using the second order sub-parametric transformations (parabolic arcs) of Eq. (6) for all the order triangular elements. Hence, we get a linear bivariate polynomial as Jacobian for all these higher order sub-parametric transformations as in Eq. (7); See Rathod et al. [25]. Therefore, substantial computational cost is reduced in computation of Eq. (8c). Newton-Raphson method gives us a very efficient means of converging to roots of non-linear system of algebraic equations, if we have a sufficiently good initial guess for the initial approximations for all the unknown velocities at nodes, but it's very difficult to guess for the present problem. Hence, we use a quasi-linearization and Gauss-Seidel iteration method to solve the system of non-linear algebraic equations in Eq. (10) and we have given single initial value guess for all the unknown velocities at nodes and we set $\mathrm{Tol} = 10^{-6}$. The computation for cross-section with 8 triangular elements for the cross-sections of Fig. 1b, is depicted in Fig. 6. We have used sub-parametric quadratic, cubic, quartic and quintic order triangular elements as in Figs. 2-5 to do the computational experiment. To track the convergence of the solution for the present problem, some common nodal points are picked. The coding for the designed algorithm is done in Mathematica 7.0.

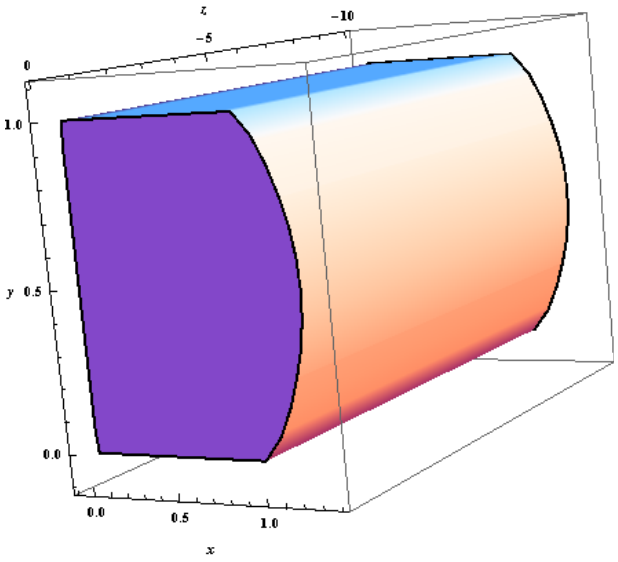

Figure 1a. Schematic of physical configuration.

Figs. 2–5 show the mapping of various curved triangles used in the computations into straight triangles. We now discuss the results depicted by the Figs.7a–7f. It is observed that the velocity of the fluid through channel increases when the Forchheimer number F is zero, which is the solution of the

Darcy–Brinkman equation (linear PDE). In Figs. 7a–7f we clearly see the effect of non-linear form drag on the velocity, which is represented by the Forchheimer number F. The velocity decreases as the Forchheimer number F increases for fixed values of Brinkman number Λ and Darcy number σ which are depicted in Figs. 7b and 7d. Similarly, the velocity decreases as the Darcy number σ increases for fixed values of Brinkman number Λ and Forchheimer number F which is depicted in Figs. 7b and 7e or Figs. 7d and 7f. Therefore, the effect of increasing F is to decrease the velocity which is similar to the effect of increasing Darcy number σ. Comparing the results in Figs. 7a–7c, we may make the inference on the effect of Brinkman number Λ on the flow. All results obtained here are in good agreement with the results of Givler and Altobelli [13]. The excellent results on the boundary and inertia effects on flow velocity speak about the utility of the method in capturing detailed flow features. It is important to mention here that the method succeeds in giving the required solution for some parameters' combination when shooting technique, based on Runge-Kutta-Fehlber45 and modified Newton-Raphson methods, fails for large values of F.

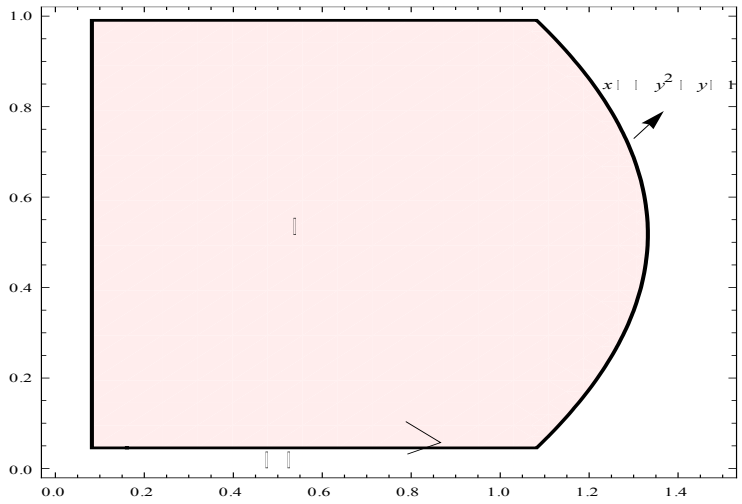

Figure 1b. Cross-section of Figure 1a.

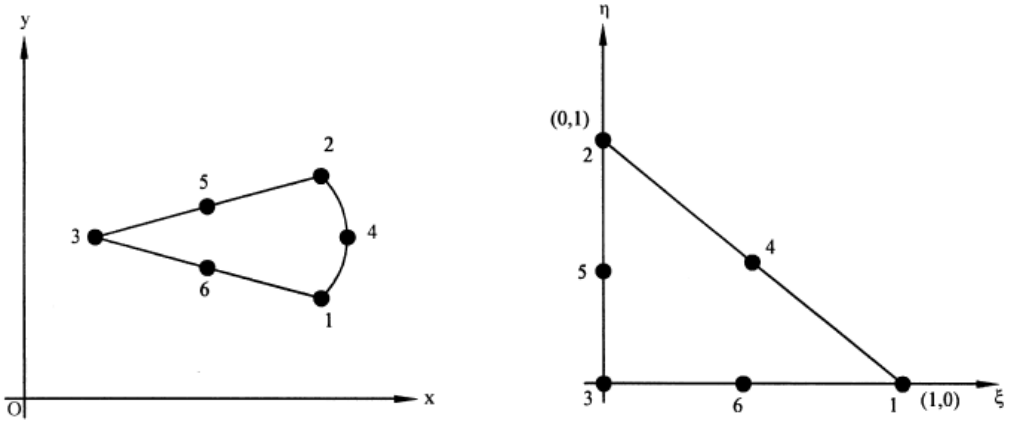

(a)Unmapped quadratic triangle (b) mapped quadratic triangle

Figure 2. Mapping of a 6-node quadratic curve triangle into standard triangle.

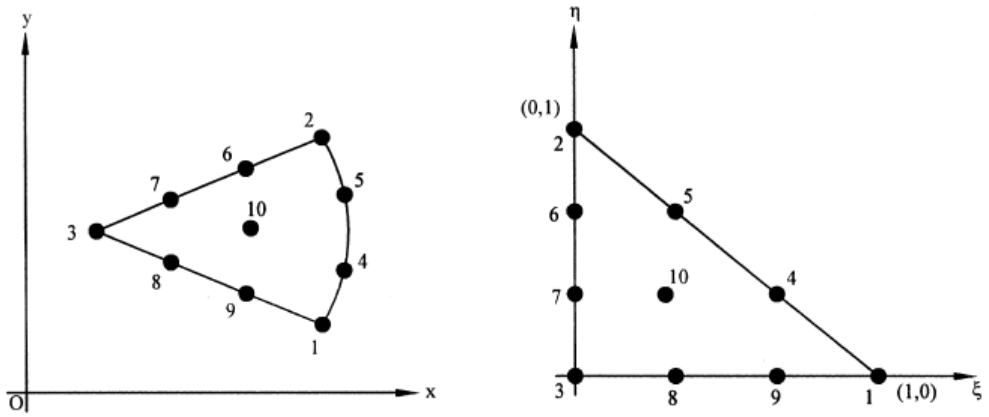

(a)Unmapped cubic triangle (b) mapped cubic triangle

Figure 3. Mapping of a 10-node cubic curve triangle into standard triangle.

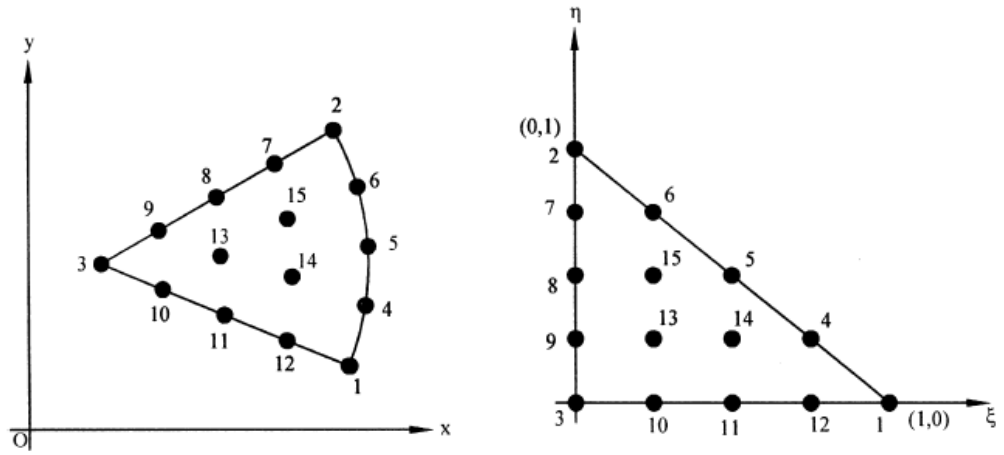

(a)Unmapped quartic triangle (b) mapped quartic triangle

Figure 4. Mapping of a 15-node quartic curve triangle into standard triangle.

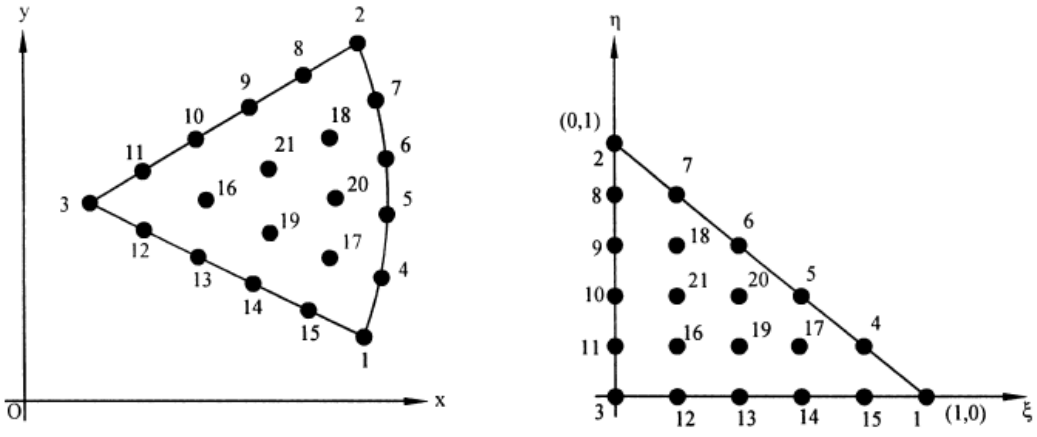

(a)Unmapped quintic triangle (b) mapped quintic triangle

Figure 5. Mapping of a 21-node quintic curve triangle into standard triangle.

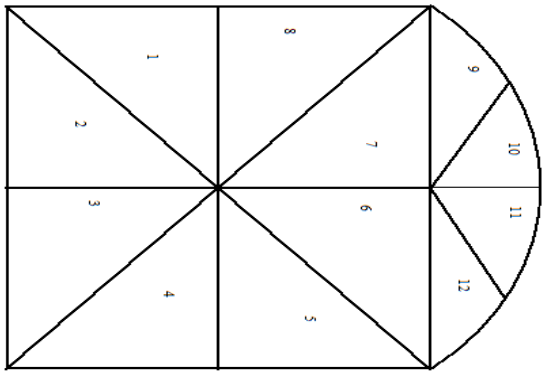

Figure 6. Description of the 12-element domain descretization of Fig. 1b.

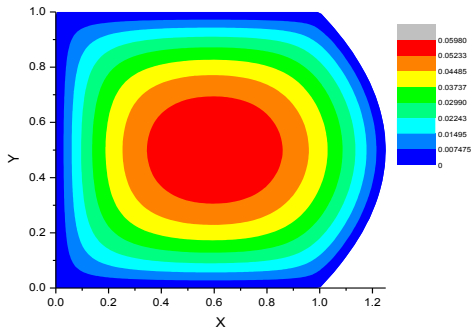

Figure 7a. Contour plot for $\Lambda = 0.8,\ \sigma^2 = 5,\ F = 50$.

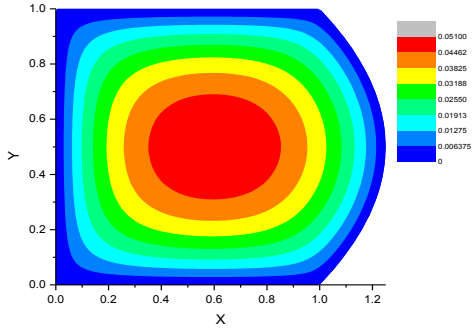

Figure 7b. Contour plot for $\Lambda = 1,\ \sigma^2 = 5,\ F = 50$.

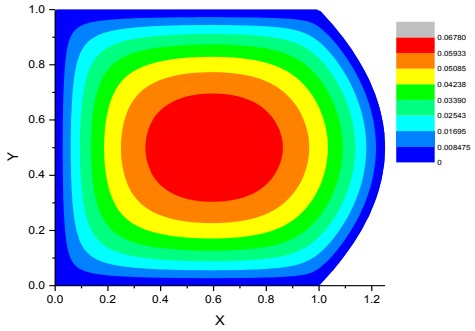

Figure 7c. Contour plot for $\Lambda = 1.2,\ \sigma^2 = 5,\ F = 50$.

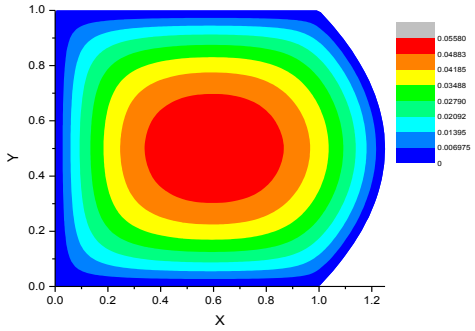

Figure 7d. Contour plot for $\Lambda = 1,\ \sigma^2 = 5,\ F = 100$.

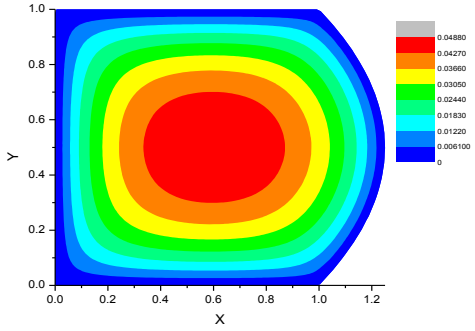

Figure 7e. Contour plot for $\Lambda = 1,\ \sigma^2 = 10,\ F = 50$.

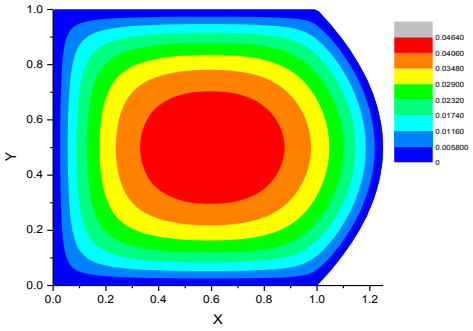

Figure 7f. Contour plot for $\Lambda = 1,\ \sigma^2 = 10,\ F = 100$

4. Conclusions

- The non-linear partial differential Eq. (1) is solved by finite element approach The resulted system of equations is naturally non-linear and the solution is obtained by quasi-linearization and a simple iterative Gauss-Seidel method.
- The method is implemented using the mathematical programming package (Mathematica 7.0)
- The errors are fairly divided among all the nodes by the present finite element method.
- The desired accuracy of 10^{-5} in the solution is obtained by the quintic order curved triangular element.
- The present method of finite element can be easily applied to many other practical and complex curved domains also.
- We wish that the present method gives us the required motivation in the usage of the sub-parametric higher order triangular elements.

Nomenclature

B^e	Column Matrix for element e
B_i^e	Elements in Column Matrix B^e
C_b	Form-drag coefficient (nondimensional)
D^e	Square matrix for element e
$D_{i,j}^e$	Elements in square Matrix D^e
E^e	Column Matrix for element e
E_i^e	Elements in Column Matrix E^e
F	Forchheimer number, $\Lambda C_b \operatorname{Re}\sigma$
G^e	Square matrix for element e
$G_{i,j}^e$	Elements in square Matrix G^e
H^e	Square matrix for element e
$H_{i,j}^e$	Elements in square Matrix H^e
h	Half channel width
J^e	Jacobian for element e

K	Permeability
N_i	Lagrange shape function at node i
p	Pressure
P	$P = \frac{ph}{\mu u_R}$
Re	Reynolds number
u	Velocity of the fluid
u_R	Characteristic velocity
U	Dimensionless velocity, $\frac{u}{u_R\left(-\frac{dP}{dZ}\right)}$
x, y, z	Global space coordinates
X	$X = \frac{x}{h}$
Y	$Y = \frac{y}{h}$
Z	$Z = \frac{z}{h}$
$-\frac{dp}{dz}$	Constant applied pressure gradient

Greek Symbols

Λ	Brinkman number, $\frac{\mu}{\mu'}$
Ω	Interior of the actual domain
Ω_e	Interior of the element
$\partial\Omega$	Boundary of the actual domain
ξ, η	Local coordinates
μ	Dynamic viscosity
μ'	Actual viscosity
ρ	Density of the fluid
σ	Porous parameter, $\frac{h}{\sqrt{\mathrm{K}}}$

Subscripts

i, j	Indices

Superscripts

e	Element number

References

[1] D. A. Nield, A. Bejan, Convection in Porous Media, Springer Verlag, New York, 2006.
[2] K. Vafai, Hand Book of Porous Media, CRC Press, 2005.
[3] N. Rudraiah, P. G. Siddheshwar, D. Pal, D. Vortmeyer, Non-Darcy effects on transient dispersion in porous media, ASME Proc., Nat. Heat Trans. Conf., Houston, Texas, USA (Ed. H. R. Jacobs), HTD – 96 (1988) 623–629.
[4] E. Skjetne, J. L. Auriault, New insights on steady, non-linear flow in porous media, Eur. J. Mech. B/Fluids, 18 (1999) 131–145.
[5] V. V. Calmidi, R. L. Mahajan, Forced convection in high porosity metal foams, ASME J. Heat Trans., 122 (2000) 557–565.
[6] A. R. A. Khaled, K. Vafai, The role of porous media in modeling flow and heat transfer in biological tissues, Int. J. Heat Mass Trans., 46 (2003) 4989–5003.
[7] J. I. Ramos, Upstream boundary conditions for flows in porous channels, Appl. Math. Comput., 93 (1998) 149–154.
[8] K. Vafai, S. J. Kim, Forced convection in a channel filled with a porous medium: An exact solution. ASME J. Heat Trans., 111 (1989) 1103–1106.
[9] D. A. Nield, S. L. M. Junqueira, J. L. Lage, Forced convection in a fluid-saturated porous medium channel with isothermal or isoflux boundaries, J. Fluid Mech., 322 (1996) 201–214.
[10] P. H. Forchheimer, Wasserbewegug durch Buden, Ver. Deutsch. Z. Ing 45 (1901)1782–1788.
[11] S. Ergun, Fluid flow through packed columns, Chem. Eng. Prog., 48 (1952) 89–94.
[12] G. Lauriat, V. Prasad, Natural convection in a vertical porous cavity: A numerical study for Brinkman extended Darcy formulation, J. Heat Trans., 109 (1987) 295–330.
[13] R. C. Givler, S. A. Altobelli, A determination of the effective viscosity for the Brinkman–Forchheimer flow model, J. Fluid Mech., 258 (1994) 355–370.
[14] D. Poulikakos, K. Renken, Forced convection in a channel filled with porous medium, including the effect of flow inertia, variable porosity and Brinkman friction, ASME J. Heat Trans., 109 (1987) 880–888.
[15] M. Parang, M. Keyhani, Boundary and inertia effect on flow and heat transfer in porous media, Int. J. Heat Mass Trans., 24 (1987) 195–203.
[16] K. Hooman, A perturbation solution for forced convection in a porous saturated duct, J. Comput. Appl. Math. 211 (2008) 57–66.
[17] K. Hooman, H. Gurgenci, A theoretical analysis of forced convection in a porous saturated circular tube: Brinkman–Forchheimer model, Trans. Porous Med., 69 (2007) 289–300.
[18] R. Sharma, R. Bhargava, I. V. Sing, Combined effect of magnetic field and heat absorption on unsteady free convection and heat transfer flow in a micropolar fluid past a semi-infinite moving plate with viscous dissipation using element free Galerkin method, Appl. Math. Comput., 217 (2010) 308–321.
[19] F. M. Allan, M. H. Hamdan, Fluid mechanics of the interface region between two porous layers, Appl. Math. Comput., 128 (2002) 37–43.
[20] I. Ergatoudis, B. M. Irons, O. C. Zienkiewicz, Curved isoparametric quadrilateral finite element analysis, Int. J. Solids Struct., 4 (1968) 31–42.
[21] O. C. Zienkiewicz, The finite Element Method in Structural and Continuum Mechanics, McGraw-Hill, New York, 1967.
[22] R. J. Y. McLeod, A. R. Mitchell, The use of parabolic arcs in matching curved boundaries in the finite element method, J. Inst. Math. Appl., 16 (1975) 239–246.
[23] H. T. Rathod, Md. Shajedul Karim, Synthetic division based integration of rational functions of bivariate polynomial numerators with linear denominators over a unit triangle $\{0 \le \xi, \eta \le 1,\ \xi + \eta \le 1\}$ in the local parametric space (ξ, η), Comput. Meth. Appl. Mech. Eng., 181 (2000) 191–235.

[24] H. T. Rathod, K. V. Nagaraja, V. Kesavulu Naidu, B. Venkatesudu, The use of parabolic arcs in matching curved boundaries by point transformations for some higher order triangular elements, Fin. Elem. Anal. Des., 44 (2008) 920–932.
[25] K. J. Bathe, Finite Element Procedures, MIT press, Cambridge (MA), Englewood Cliffs, NJ, 1996.
[26] O. C. Zienkiewicz, R. L. Taylor, J. Z. Zhu, The Finite Element Method: Its Basis and Fundamentals, 6th ed., Oxford: Elsevier, 2005.
[27] M. A. Bhatti, Fundamental Finite Element Analysis and Applications, John Wiley & Sons, Inc., New York, 2005.
[28] M. Mofid, A. Vafai, K. Farahani, Finite element solution of Dirichlet's nonlinear partial differential equation with mixed boundary conditions, Comput. Methods Appl. Mech. Engrg. 169 (1999) 81–88.
[29] Murali K, V. Kesavulu Naidu and B. Venkatesh, " Optimal subparametric finite element approach for a Darcy-Brinkman fluid flow problem through a rectangular channel with one curved side", IOP Conf. Series: Materials Science and Engineering 310 (2018) 012145
[30] H. T. Rathod, K. V. Nagaraja, B. Venkatesudu, N. L. Ramesh, Gauss Legendre quadrature over a triangle, J. Indian Inst. Sci., 84 (2004) 183–188.
[31] H. T. Rathod, K. V. Nagaraja, B. Venkatesudu, Symmetric Gauss Legendre quadrature formulas for composite numerical integration over a triangular surface, Appl. Math. Comput., 188 (2007) 865–876.
[32] J.C.Umavathi, Odelu Ojjel, K.Vajravelu, Numerical analysis of natural convective flow and heat transfer of nanofluids in a vertical rectangular duct using Darcy-Forchheimer-Brinkman model, Int. journal of Thermal Sciences, vol. 111, Jan 2017, 511-524.
[33] TaseerMuhammad, AhmedAlsaedi, TasawarHayata, Sabir AliShehzad, A revised model for Darcy-Forchheimer three-dimensional flow of nanofluid subject to convective boundary condition, Results in Physics, Vol. 7, 2017, 2791-2797.